

Miniaturized Dual-Band Wi-Fi Antenna for Mobile Application

Maizatul Alice Meor Said¹, Ang Wy Ruenn¹, Mohamad Harris Misran¹, Mohd Azlishah Othman¹, Shadia Suhaimi², Nurmala Irdawaty Hassan³, Amyrul Azuan Mohd Bahar⁴

¹Centre for Telecommunication Research & Innovation (CeTRI), Fakulti Teknologi dan Kejuruteraan Elektronik dan Komputer (FTKEK), Universiti Teknikal Malaysia Melaka (UTeM), Hang Tuah Jaya, 76100 Durian Tunggal, Melaka, Malaysia, ²Faculty of Business, Multimedia University, Jalan Ayer Keroh Lama, 75450 Bukit Beruang, Melaka MALAYSIA, ³Electrical & Electronic Engineering Programme, School of Engineering and Physical Sciences, Heriot-Watt University Malaysia, No. 1, Jalan Venna P5/2, Precinct 5, 62200 Putrajaya, Malaysia, ⁴Intel Corporation Sdn. Bhd., Bayan Lepas, Pulau Pinang, Malaysia
Corresponding Author Email: maizatul@utem.edu.my

To Link this Article: <http://dx.doi.org/10.6007/IJARBS/v14-i10/23124> DOI:10.6007/IJARBS/v14-i10/23124

Published Date: 05 October 2024

Abstract

This thesis addresses the growing demand for compact and efficient dual-band Wi-Fi antennas operating at both 2.4 GHz and 5 GHz frequencies. Miniaturized dual-band Wi-Fi antenna for mobile application is a collaboration project between UTeM and Intel to design a compact dual-band antenna in mobile application such as smartphones, tablets, and laptops. The objective of this research is to design and optimize a miniaturized dual-band Wi-Fi antenna, operating at 2.4 GHz and 5 GHz, to meet the requirements of compact electronic devices. The scope of this study encompasses the design, simulation, fabrication, and testing of a meander line antenna for dual-band Wi-Fi applications. Meander line antennas are chosen for their ability to achieve compactness and multiband operation. The methodology involves a comprehensive study of meander line antenna configurations, parametric analysis, and optimization to achieve desired performance metrics. The antenna is fabricated and experimentally tested to validate simulation results and assess real-world performance. Measurements are conducted to evaluate parameters such as return loss, radiation pattern, and antenna gain. The research contributes to the ongoing efforts in antenna design for modern communication systems, addressing the challenges posed by size constraints in emerging electronic devices.

Keywords: Miniaturized, Dual-Band, Meander Line

Introduction

The proliferation of mobile devices and the increasing demand for wireless connectivity have reshaped the way we communicate, access information, and interact with the digital world. Wi-Fi technology has emerged as a vital solution for wireless internet access and local network connectivity, enabling seamless communication and data transfer in various environments (Othman, 2023; Islam et al., 2022). However, the design and implementation of Wi-Fi antennas for mobile applications present unique challenges that must be addressed to meet the growing demands of users (Kaushik et al., 2021; Rao, 2022; Misran et al., 2024).

Mobile devices, such as smartphones, tablets, and wearables, have become essential companions in our everyday lives. These devices require compact and space-efficient antennas to provide reliable wireless connectivity while occupying minimal physical space (Ghaffar et al, 2018; Anusha, Deepak, 2022). However, designing antennas for mobile applications is a complex task due to the limitations imposed by the small form factor, multi-band operation, and the need to maintain high performance in terms of gain, bandwidth, and radiation efficiency (Kaplan and Göçen, 2022; Soltani et al., 2017; Lauder and Sun, 2020).

The miniaturization of antennas has been a subject of extensive research to overcome these challenges. Researchers have explored various miniaturization techniques, such as compact antenna geometries and advanced materials, to reduce the physical size of antennas without compromising their performance (Khade et al., 2023; Zhang et al., 2023; Karthik, 2015). These techniques aim to achieve compactness, multi-band operation, and efficiency in mobile Wi-Fi antennas (Pozar and Kaufman, 1988; Diman et al., 2021; Botau and Negrea, 2022; Faza et al., 2019).

Method

The MLA line is designed in CST Studio Suite 2022, the antenna consists of dielectric, meandered line patch and ground patch. Figure 1(a) and Figure 1(b) show the front and back view of the MLA. The port is constructed at the end of the transmission line as illustrated in Figure 1(c).

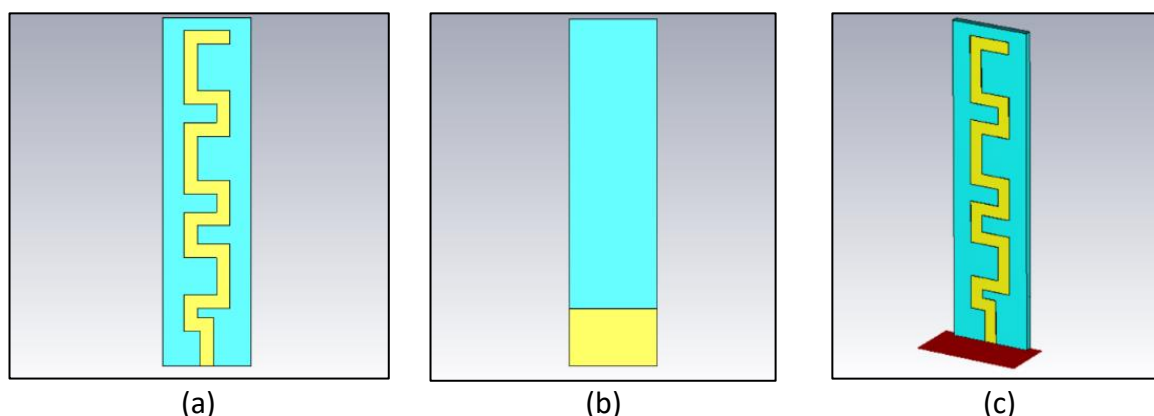


Figure 1: Proposed MLA (a) Front view (b) Back view and (c) Port constructed at the end of transmission line

Calculation of the Parameters

Calculation should be done first to find the dimension of the substrate, patch, inset and port of the antenna. For designing of a microstrip patch antenna, the resonant frequency and a dielectric medium for which antenna is to be designed has to be selected. The parameters to be calculated are as below:

1 Width of the patch [21]:

$$W = \frac{c}{2f_0 \sqrt{\frac{\epsilon_r + 1}{2}}} \quad (2.1)$$

2 Effective Dielectric Constant [21]:

$$\epsilon_{eff} = \frac{\epsilon_r + 1}{2} + \frac{\epsilon_r - 1}{2} \left(\frac{1}{\sqrt{1 + 12 \left(\frac{h}{W} \right)}} \right) \quad (2.2)$$

3 Effective Length [21]:

$$L_{eff} = \frac{c}{2f_0 \sqrt{\epsilon_{eff}}} \quad (2.3)$$

4 Length Extension [21]:

$$\Delta L = 0.412h \left[\frac{(\epsilon_{eff} + 0.3) \left(\frac{W}{h} + 0.264 \right)}{(\epsilon_{eff} - 0.258) \left(\frac{W}{h} + 0.8 \right)} \right] \quad (2.4)$$

5 Length of the patch [21]:

$$L = L_{eff} - 2\Delta L \quad (2.5)$$

6 Input Impedance of the Antenna [21]:

$$Z_{in} = 90 \left(\frac{\epsilon_r^2}{\epsilon_r - 1} \right) \left(\frac{L}{W} \right)^2 \quad (2.6)$$

7 Bandwidth of the Antenna [21]:

$$BW = 3.77f_0 \left(\frac{\epsilon_r - 1}{\epsilon_r^2} \right) \left(\frac{Wh}{L\lambda} \right)^2 \quad (2.7)$$

Fabrication Process

The MLA antenna is fabricated by undergoing the etching process on FR-4 board. The etching process for creating an antenna on an FR-4 board involves selectively removing unwanted copper material to define the antenna structure. The copper layer on the FR-4 serves as the conductive material for the antenna. The etched FR-4 board is then cut to remove excessive dielectric part that is not in the design dimension. Finally, a SMA port is soldered onto the end of the transmission line of the MLA. Figure 2(a) and Figure 2(b) depict the fabricated MLA with SMA port soldered onto its transmission line.

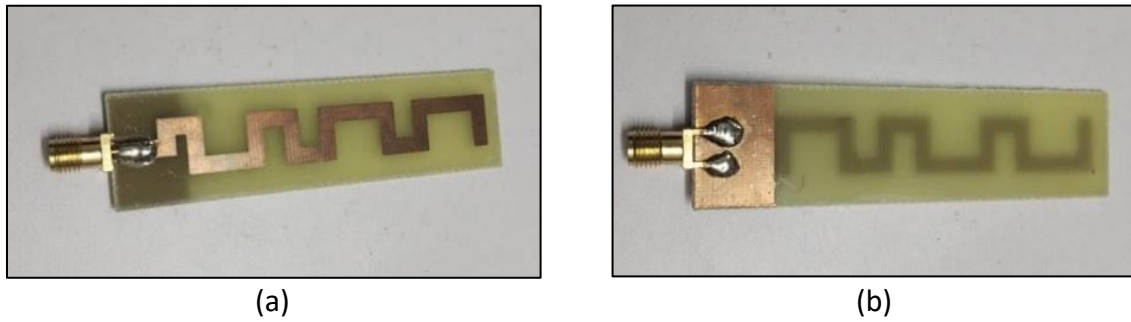


Figure 2: View of the MLA (a) Front (b) Back

Measurement Process

The fabricated MLA's return loss is measured using VNA as shown in Figure 3. The radiation pattern, gain and directivity of the antenna is measured inside chamber room. Figure 4 depicts the measurement setup of the MLA inside the chamber room.

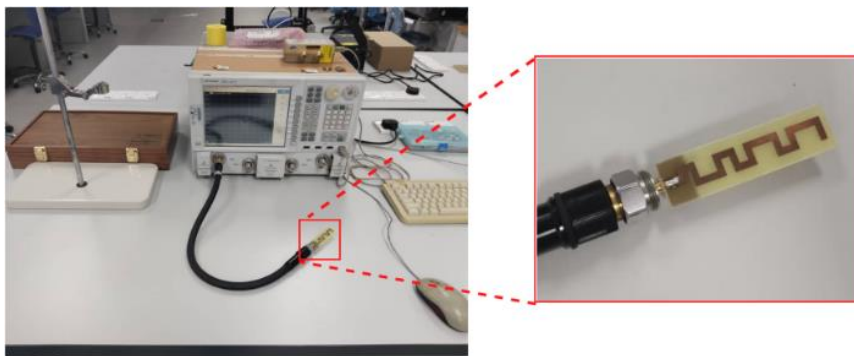


Figure 3. Measurement set up using VNA

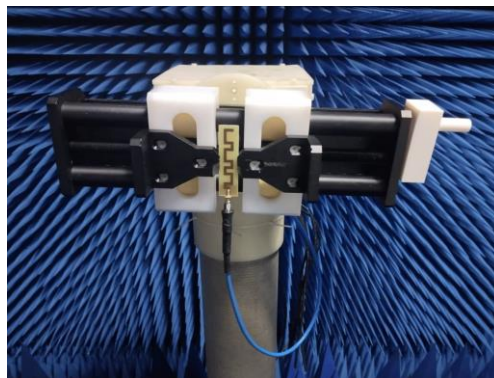


Figure 4. Gain and directivity measurement

Results and Discussion

This section marks a pivotal phase in unraveling the intricate design and performance evaluation of this design. The preceding chapters meticulously delved into the theoretical underpinnings, design considerations, and simulation methodologies employed in crafting this innovative antenna. This section presents a comprehensive analysis of the antenna's performance across the dual frequency bands, shedding light on its efficacy in meeting the demands of contemporary wireless communication systems. Through a series of carefully designed experiments and simulations, the aim is to elucidate the antenna's key parameters, such as gain, radiation pattern, impedance matching, and other relevant metrics.

Return Loss

The MLA consist of multiple section of zigzag line as shown in Figure 5. The dielectric has a thickness of 1.6mm. Each of this section will affect the return loss and gain of the antenna at resonant frequencies of 2.4GHz and 5GHz.

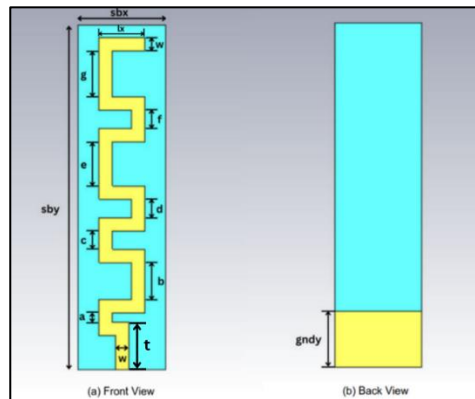


Figure 5: Parameters of Proposed MLA Design

Table 1: Parameters for the antenna

Parameter	Unit (mm)
sbx	19
sby	75
w	2.9
lx	10
a	2
b	8
c	4
d	4
e	10
f	4
g	10
t	7.5
gndy	12.3

Parametric sweep is done to observe the effect of the meander section changes towards the return loss and gain of the antenna at desired resonant frequencies as shown in Figure 6 to Figure 7. The final simulation result of return loss for designed antenna is shown in Figure 8. It shows that two operating bands are generated at 2.4 and 5 GHz frequency band. The antenna elements resonated between 2.34 – 2.47 GHz and 4.87–5.68 GHz with a minimum $|S_{11}| < -10$ dB. The optimized antenna shows the bandwidth of about 70 MHz on lower band of 2.4GHz and about 80 MHz on upper band of 5GHz that is compatible with WLAN standard. The maximum return loss for resonant frequency 2.4 GHz is -26.92 dB and 5GHz is - 45.34 dB.

Return Loss S11 vs Frequency Graph

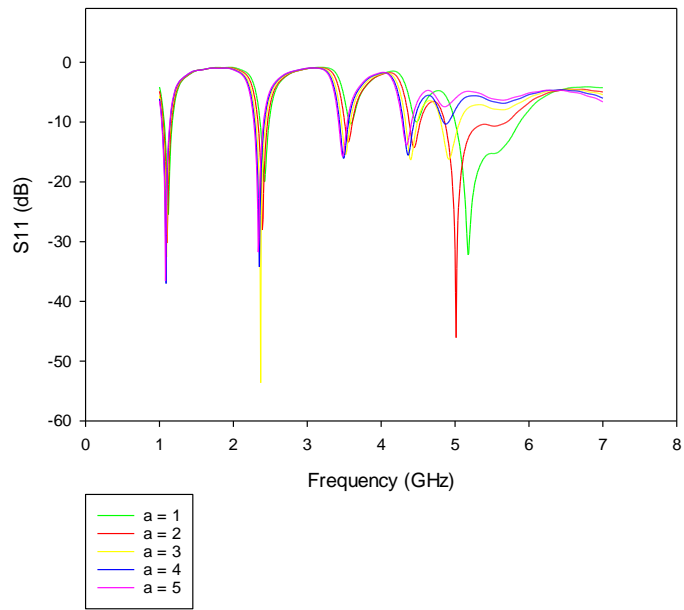


Figure 6: Parameter sweep 'a'

Return Loss vs Frequency Graph

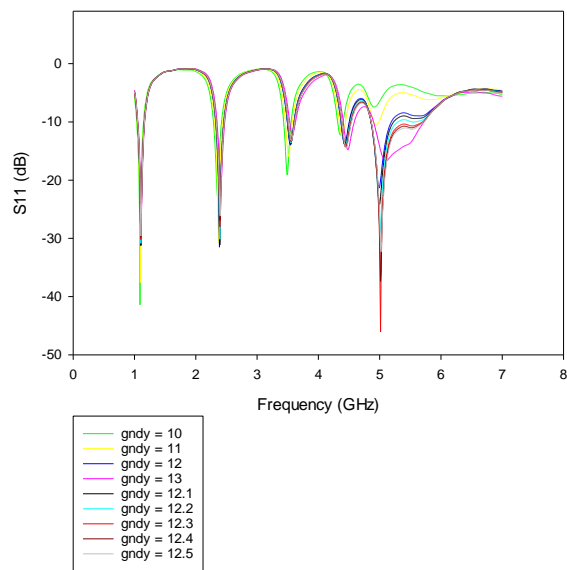


Figure 7: Parameter sweep 'gndy'

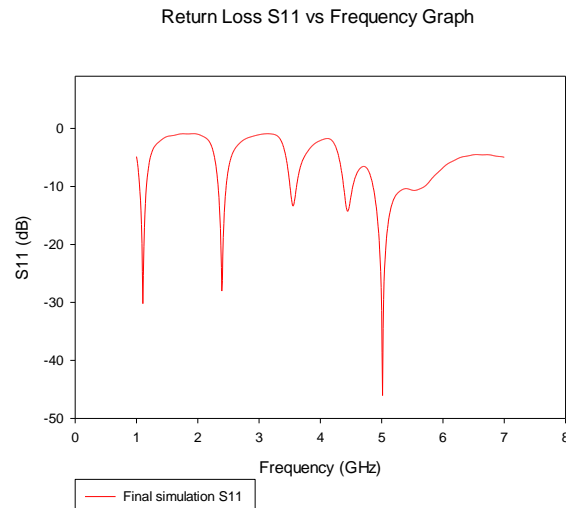


Figure 8: Final simulated S11 result for the proposed MLA

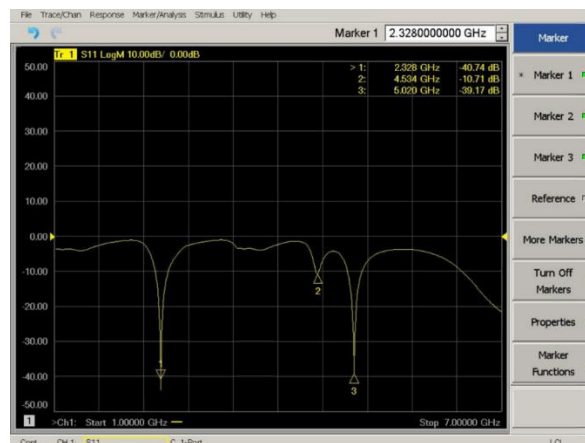


Figure 9: Return loss measurement of the fabricated MLA

As per the measured results depicted in Figure 9 the antenna has dual band response at 2.328 GHz and 5.020 GHz with S-parameter of -40.74 dB and -39.17dB. When compared to the simulated result, the return loss of upper band 5GHz of the fabricated MLA is similar to the simulated result. However, the return loss graph of the fabricated MLA is shifted to the left for the band of 2.4GHz. This is due to the flaw in the fabricated copper trace on the MLA. The dimension of the copper on the MLA may not be exactly the same as in the CST software design. The result is still considered acceptable as the bandwidth cover over 2.4 GHz.

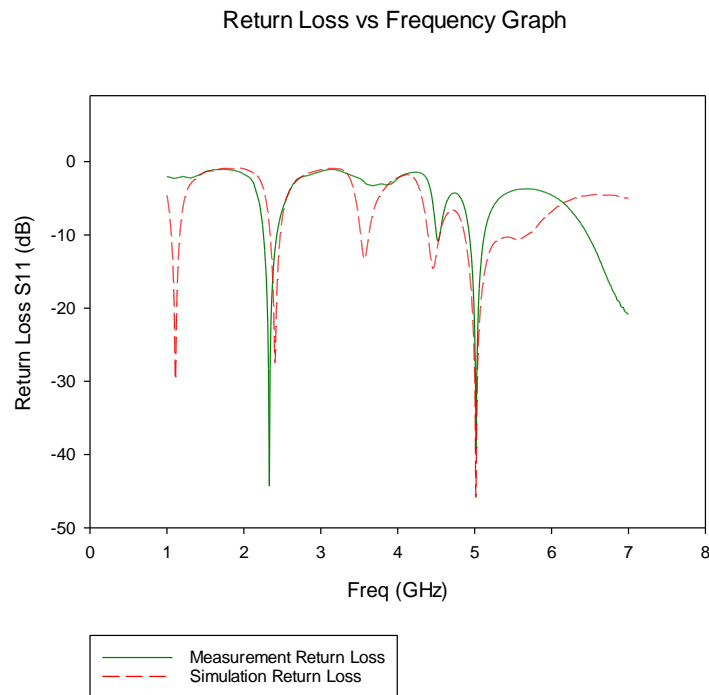


Figure 10: Comparison of S11 between simulation and measurement result

Based on the result plot, the results are similar between the simulation and measurement with slightly different due to fabrication errors such as cutting dielectric process and the SMA port soldered onto the transmission line of the MLA. The comparison graph of return loss is illustrated in Figure 10.

Reference Impedance

The impedance value at 2.4 GHz and 5GHz is 50.2 ohm as illustrated in Figure 11. Theoretically, antenna good impedance value is near 50ohm. This is because coaxial cables, which are commonly used for transmitting RF signals, are optimized for 50-ohm impedance. Hence, the result shows the proposed fabricated antenna has a good impedance value.

Reference Impedance vs Frequency Graph

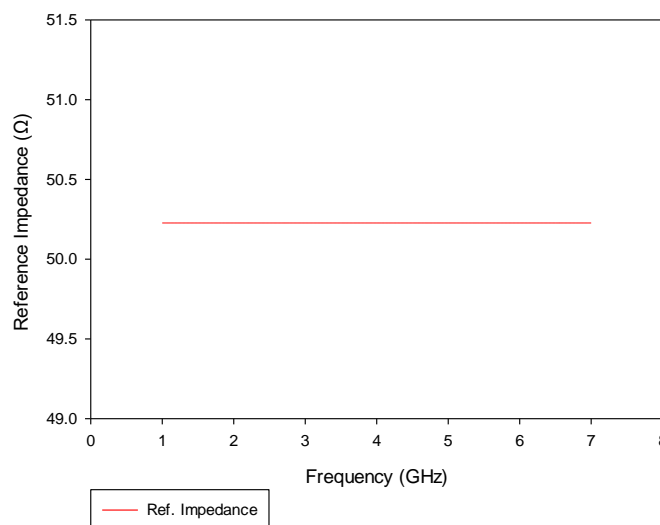


Figure 11: Reference impedance

Voltage Standing Wave Ratio Voltage

The fabricated antenna has VSWR of 1.094 and 1.059 at 2.4 GHz and 5 GHz respectively. This shows that the antenna has a good VSWR as it is closer to 1. Figure 12 indicates the VSWR plot for the MLA.

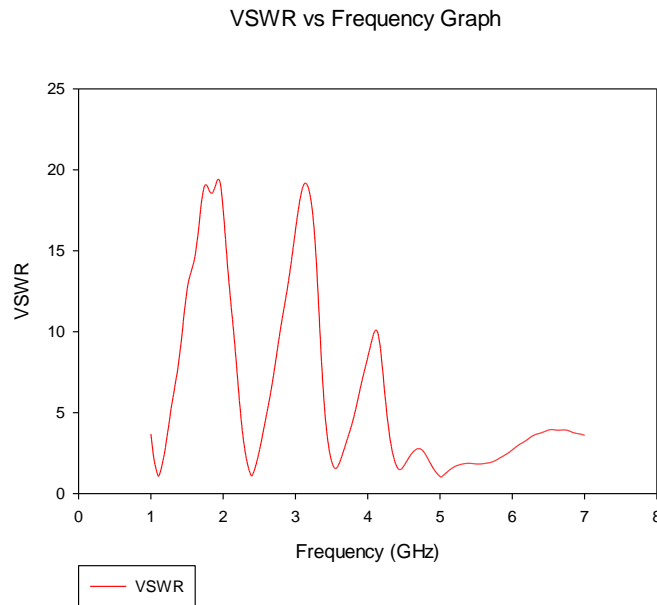


Figure 12: VSWR plot of the MLA

Radiation Pattern

Figure 13 and Figure 14 below show the radiation pattern of the MLA. Based on the farfield plot, the radiation pattern is nearly omnidirectional for both bands. Omnidirectional antennas provide a consistent signal strength, reducing the likelihood of signal dropouts as users move through different locations. In addition, mobile devices are often used in different orientations (portrait, landscape, etc.). An omnidirectional antenna ensures that the device can maintain a reliable connection regardless of how it is held or positioned. "Decibels isotropic" (dBi) is a unit of measurement commonly used in antenna engineering to express the gain of an antenna relative to an isotropic radiator. The term "isotropic" refers to an idealized point source that radiates uniformly in all directions, creating a spherical radiation pattern. Both of these band achieved the expected gain. The 1D farfield results are depicted in Figure 15(a) and Figure 15(b).

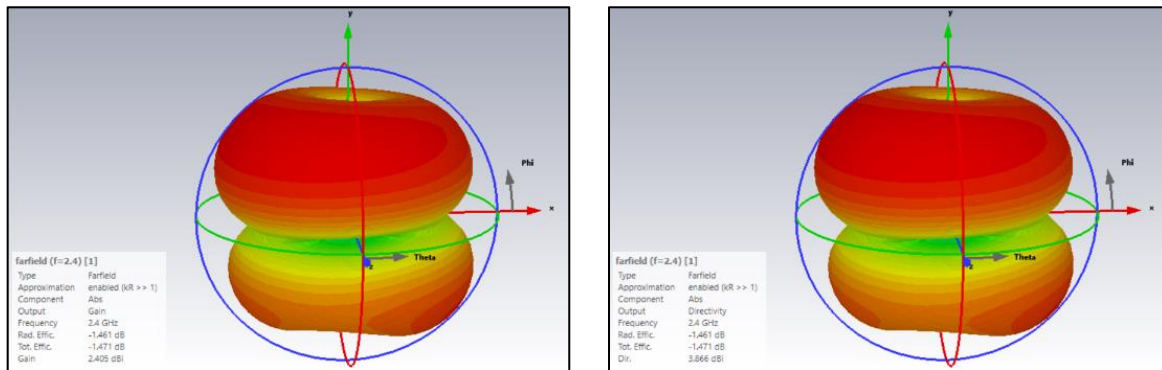


Figure 13: Radiation pattern of 2.4GHz frequency band

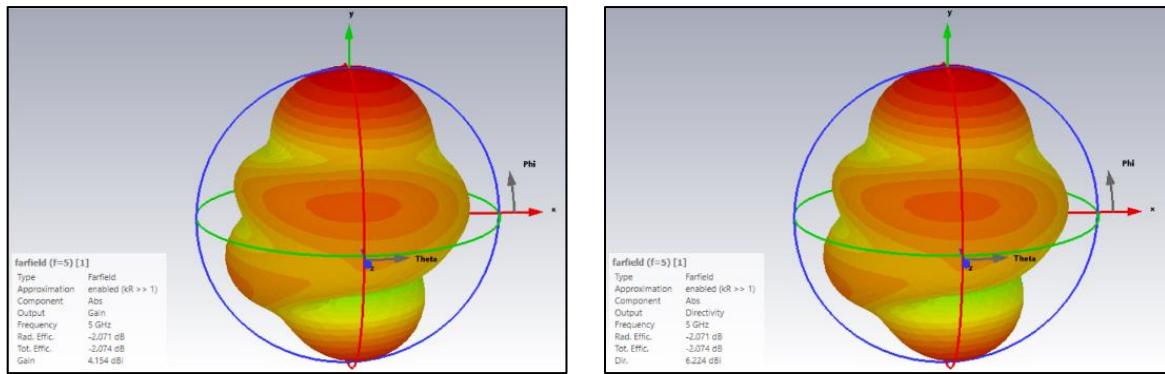


Figure 14: Radiation pattern of 5GHz frequency band

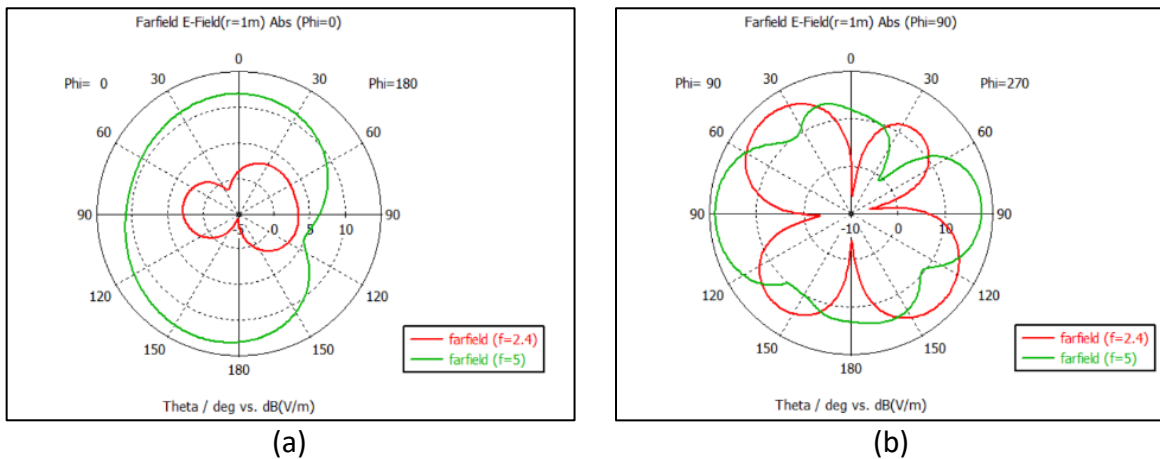


Figure 15: Radiation pattern of 5GHz frequency band (a) Phi = 0° (b) Phi = 90°

Gain

The comparison graph of simulation and measurement gain of the MLA is presented in Figure 16. The antenna yields simulation gain of 2.405 dBi at 2.4 GHz and 4.154 dBi at 5 GHz. The measurement gain of the fabricated MLA is 2.94 dBi at 2.4 GHz and 4.117 dBi at 5 GHz.

Gain vs Frequency Graph

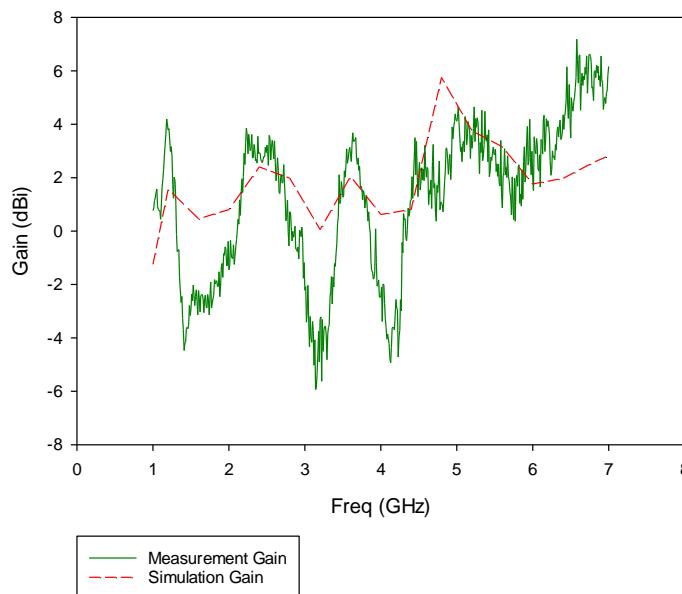


Figure 16: Comparison of gain graph

Directivity

The MLA design has directivity of 3.866 dBi for 2.4 GHz and 6.224 dBi for 5 GHz when simulated in CST software. The measurement result shows that the fabricated MLA has directivity of 4.033 dBi at 2.4 GHz and 6.752 dBi at 5 GHz. Figure 17 depicts the simulation and measurement result of the directivity of the MLA.

Frequency vs Directivity Graph

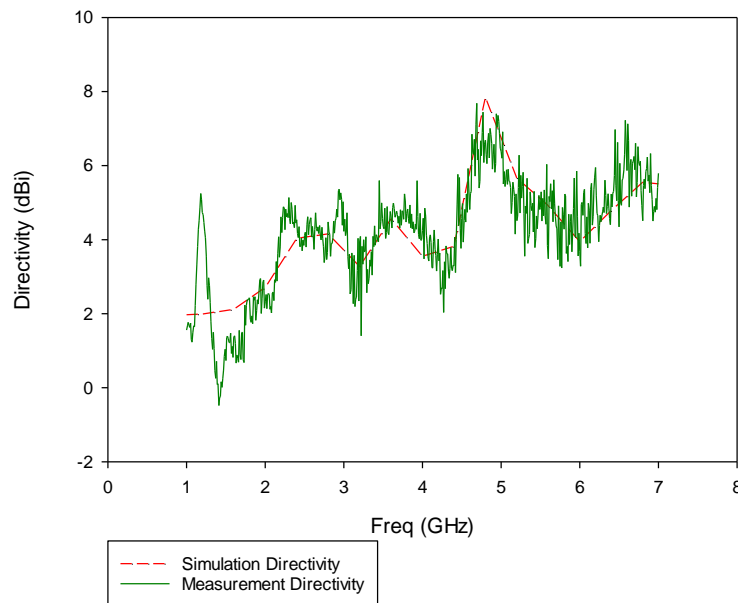


Figure 17: Comparison of directivity graph

Efficiency

Efficiency is a fundamental metric for evaluating the performance of an antenna. It provides insights into how effectively the antenna converts electrical power into radiated energy. A highly efficient antenna ensures that a significant portion of the input power is radiated as electromagnetic waves. The efficiency of the MLA can be calculated using directivity and gain of the antenna [22]:

$$\text{Efficiency, } \eta = \text{gain} / (\text{directivity}) \times 100\%$$

Simulation result:

Efficiency for 2.4GHz:

$$\eta = \frac{2.405}{3.866} \times 100\%$$

$$\eta = 62\%$$

Efficiency for 5GHz:

$$\eta = \frac{4.154}{6.224} \times 100\%$$

$$\eta = 67\%$$

Efficiency for measurement result:

Efficiency for 2.4GHz:

$$\eta = \frac{2.94}{4.033} \times 100\%$$

$$\eta = 73\%$$

Efficiency for 5GHz:

$$\eta = \frac{4.117}{6.752} \times 100\%$$

$$\eta = 61\%$$

Comparison of Result

The overall comparison result between simulation and measurement is expressed in Table 2. Based on the table, the simulation antenna performs better at 5 GHz than 2.4 GHz while the fabricated antenna performs better at lower frequency 2.4 GHz.

Table 2

Comparison between parameters of measurements and simulations

Freq (GHz)	Type of results	S₁₁ (dB)	Gain (dBi)	Directivity (dBi)	Efficiency (%)
2.4	Simulation	-26.92	2.405	3.866	62
	Measurement	-40.74	2.94	4.033	73
5	Simulation	-45.35	4.154	6.224	67
	Measurement	-39.17	4.117	6.752	61

Analysis of Current and Recent Research

Table 3 shows the comparison of recent literature review. From the table, it can be observed that the antenna has a trade-off between the size and the gain. The proposed work design is to minimize the dimension of the size while maintaining a good return loss and high gain to increase its efficiency.

Table 3

The Recent Literature Concerning The Proposed Design

Ref.	Dimension (mm ³)	Frequency (GHz)	S ₁₁ (dB)	Gain (dBi)
[15]	46 × 20 × 1.6	2.4	-15	0.5
		5	-27	2.5
[16]	18 × 12 × 1.5	2.4	-23	-
		5	-14	-
[17]	25 × 45 × 1.6	2.4	-25	1.15
		5	-35	4.75
[18]	10 × 50 × 0.8	2.4	-31.17	1.918
		5	-42.05	2.303
[19]	30 × 30 × 1.6	2.4	-34.88	2.99
		5	-12.56	1.25
[20]	50 × 150 × 11.1	2.4	-28	8.4
		5	-32	7
This work	19 × 75 × 1.6	2.4	-40.74	2.94
		5	-39.17	4.117

Conclusion

In summary, this project has successfully achieved compact antenna size with good return loss and gain at desired resonant frequency. The antenna achieved resonant frequencies at 2.328 GHz and 5.020 GHz with S-parameter of -40.74 dB and -39.17 dB. It also possesses desirable gain at both resonant frequencies where 2.4 GHz has gain of 2.94 dBi and 5 GHz yield a gain of 4.117 dBi. Furthermore, the antenna also achieved efficiency over than 60%, for both frequency bands. This reduces the overall energy consumption of the communication system, contributing to energy efficiency and sustainability. Despite the project's successes, it is essential to acknowledge its limitations. Meander line antennas are often designed for specific frequency bands, and achieving broad bandwidth can be challenging. This limitation may restrict their applicability in systems that require wide frequency coverage. Thus, future work and research may be done to improve the bandwidth of meander line antenna while maintaining its compact size and performance.

Acknowledgements

The author would like to thank the Centre for Research and Innovation Management (CRIM) UTeM, Universiti Teknikal Malaysia Melaka (UTeM), and the Malaysian Ministry of Higher Education (MOHE) for financing this work under FRGS/1/2023/TK07/UTEM/02/18.

References

- Botau, A., & Negrea, C. (2022). Thermal behavior of FR4 and flexible substrates for high output IR LEDs application. *2022 IEEE 9th Electronics System-Integration Technology Conference (ESTC)*, Sibiu, Romania, pp. 528-532. <https://doi.org/10.1109/ESTC55720.2022.9939550>
- Diman, A. A. (2021). Efficient SIW-feed network suppressing mutual coupling of slot antenna array. *IEEE Transactions on Antennas and Propagation*, 69(9), 6058-6063.
- Syahirah, F. (2019). Dual-band aperture coupled antenna with harmonic suppression capability. *Telkomnika Telecommunication Computing Electronics and Control*, 17(1). <https://doi.org/10.12928/TELKOMNIKA.v17i1.11598>
- Ghaffar, A., Li, X. J., & Seet, B.-C. (2018). Compact dual-band broadband microstrip antenna at 2.4 GHz and 5.2 GHz for WLAN applications. *2018 IEEE Asia-Pacific Conference on Antennas and Propagation (APCAP)*, Auckland, New Zealand, pp. 198-199. <https://doi.org/10.1109/APCAP.2018.8538297>
- Islam, T., Rutan-Bedard, S. I., & Roy, S. (2022). On the study of a low profile triple-band meander line antenna for wireless applications. *2022 IEEE International Symposium on Antennas and Propagation and USNC-URSI Radio Science Meeting (AP-S/URSI)*, pp. 1812-1813. <https://doi.org/10.1109/AP-S/USNC-URSI47032.2022.9887121>
- Kaplan, Y., & Göçen, C. (2022). A dual-band antenna design for 2.4 and 5 GHz Wi-Fi applications. *Avrupa Bilim ve Teknoloji Dergisi*, (34), 685-688. <https://doi.org/10.31590/ejosat.1084161>
- Kaushik, M., Dhanoa, J. K., & Khandelwal, M. K. (2021). Meander line based two port MIMO small antenna for UHF RFID and Sub-6 GHz applications. *2021 IEEE International Conference on RFID Technology and Applications (RFID-TA)*, pp. 219-222. <https://doi.org/10.1109/RFID-TA53372.2021.9617323>
- Karthick, M. (2015). Design of 2.4GHz patch antennae for WLAN applications. *2015 IEEE Seventh National Conference on Computing, Communication and Information Systems (NCCCIS)*, Coimbatore, India, pp. 1-4. <https://doi.org/10.1109/NCCCIS.2015.7295902>
- Khade, S. S., Tembhare, S., Gawali, P., Jain, S., Ingole, R., & Bawankar, C. V. (2023). Dual band meander line antenna for 5G and WLAN application. *2023 International Conference on Computer, Electronics & Electrical Engineering & their Applications (IC2E3)*, Srinagar Garhwal, India, pp. 1-5. <https://doi.org/10.1109/IC2E357697.2023.10262496>
- Lauder, D., & Sun, Y. (2020). An overview of automatic antenna impedance matching for mobile communications. *2020 European Conference on Circuit Theory and Design (ECCTD)*, Sofia, Bulgaria, pp. 1-4. <https://doi.org/10.1109/ECCTD49232.2020.9218350>
- Misran, M. H., Meor Said, M. A., Othman, M. A., Jaafar, A. S., Abd Manap, R., Suhaimi, S., & Hassan, N. I. (2024). DGS based CP antenna for 5G communication with harmonic. *International Journal of Integrated Engineering*, 16(1), 301-311. <https://doi.org/10.30880/ijie.2024.16.01.025>
- Othman. (2023). 3.5 GHZ Vivaldi antennas: A comprehensive parametric analysis for unleashing 5G communication technology. *ASEAN Engineering Journal*, 13(3), 159-163. <https://doi.org/10.11113/aej.v13.19774>
- Pozar, D. M., & Kaufman, B. (1988). Comparison of three methods for the measurement of printed antenna efficiency. *IEEE Transactions on Antennas and Propagation*, 36(1), 136-139. <https://doi.org/10.1109/8.1084>
- Rao, N. (2022). Modified Sierpinski and its use in fractal patch antenna for miniaturization and multiband behavior. *2022 IEEE Microwaves, Antennas, and Propagation Conference*

- (MAPCON), Bangalore, India, pp. 1804-1809.
<https://doi.org/10.1109/MAPCON56011.2022.10047750>
- Soltani, S., Lotfi, P., & Murch, R. D. (2017). A dual-band multiport MIMO slot antenna for WLAN applications. *IEEE Antennas and Wireless Propagation Letters*, 16, 529-532.
<https://doi.org/10.1109/LAWP.2016.2587732>
- Syahirah, F. (2019). Dual-band aperture coupled antenna with harmonic suppression capability. *Telkomnika Telecommunication Computing Electronics and Control*, 17(1).
<https://doi.org/10.12928/TELKOMNIKA.v17i1.11598>
- Zhang, W., Li, Y., Wei, K., & Zhang, Z. (2023). Dual-band decoupling for two back-to-back PIFAs. *IEEE Transactions on Antennas and Propagation*, 71(3), 2802-2807.
<https://doi.org/10.1109/TAP.2023.3234175>